

Polysulfone/poly(ether sulfone) blended membranes for CO₂ separation

Hafiz Abdul Mannan,¹ Hilmi Mukhtar,¹ Maizatul Shima Shaharun,² Mohd Roslee Othman,³ Thanabalan Murugesan¹

¹Department of Chemical Engineering, Universiti Teknologi Petronas, Bandar Seri Iskandar, Perak 32610, Malaysia

²Department of Fundamental and Applied Sciences, Universiti Teknologi Petronas, Bandar Seri Iskandar, Perak 32610, Malaysia

³School of Chemical Engineering, Universiti Sains Malaysia, 11800 USM, Pulau Pinang, Malaysia

Correspondence to: H. Mukhtar (E-mail: hilmi_mukhtar@petronas.com.my)

ABSTRACT: Polymer blending as a modification technique is a useful approach for augmenting the gas-separation and permeation properties of polymeric membranes. Polysulfone (PSF)/poly(ether sulfone) (PES) blend membranes with different blend ratios were synthesized by conventional solution casting and solvent evaporation technique. The synthesized membranes were characterized for miscibility, morphology, thermal stability, and spectral properties by differential scanning calorimetry (DSC), field emission scanning electron microscopy, thermogravimetric analysis, and Fourier transform infrared (FTIR) spectroscopy, respectively. The permeation of pure CO₂ and CH₄ gases was recorded at a feed pressure of 2–10 bar. The polymer blends were miscible in all of the compositions, as shown by DSC analysis, and molecular interaction between the two polymers was observed by FTIR analysis. The thermal stability of the blend membranes was found to be an additive property and a function of the blend composition. The morphology of the blend membranes was dense and homogeneous with no phase separation. Gas-permeability studies revealed that the ideal selectivity was improved by 65% with the addition of the PES polymer in the PSF matrix. The synthesized PSF/PES blend membranes provided an optimized performance with a good combination of permeability, selectivity and thermal stability. © 2015 Wiley Periodicals, Inc. *J. Appl. Polym. Sci.* **2016**, *133*, 42946.

KEYWORDS: blends; membranes; phase behavior; separation techniques

Received 4 December 2014; accepted 15 September 2015

DOI: 10.1002/app.42946

INTRODUCTION

The separation of gas mixtures with polymeric membranes is a proven industrial separation process. Membrane-based gas separation is a combination of membrane material, module, and process design, and research is ongoing in all of these areas of membrane technology.¹ The performance of a membrane is rated on the basis of permeability (transport factor) and selectivity (separation factor).² Cellulose acetate is usually taken as a benchmark for natural gas processing plants with a selectivity of 10–15.³ It has been shown that polymeric materials follow a general tradeoff between permeability and selectivity.⁴ When the permeability of a membrane is plotted against the selectivity, data points fall below a limiting line known as the *Robeson upper bound limit*. Thus, an improvement in the permeability is restricted by a loss in the selectivity and vice versa. Moreover, plasticization is a big challenge in polymeric membranes, and it results in a loss of performance. At high partial pressures of CO₂, polymeric membranes are prone to attack by fast-moving CO₂, and they result in the swelling of polymer chains because of the high solubility of CO₂ in the polymer matrix.⁵ The

thermal, chemical, and mechanical stability of membranes is an issue of interest for many applications.^{6,7} The durability and stability of a membrane reduces the associated costs of maintenance and repairs.

A number of modification techniques have been reported in the literature for the development of high-performance materials, such as mixed-matrix membranes, ionic-liquid-supported membranes, and polymer-blend membranes.^{8–10} In particular, polymer blending is considered a simple approach for the development of high-performance polymeric materials. The selection of a suitable polymer pair can provide additive and synergetic properties in blend materials that are not found in individual polymers. The combination of higher permeability and higher selectivity polymer pairs by polymer blending technique is expected to result in the improved performance of polymeric membranes. The ultimate separation performance of a polymer blend may surpass or move closer to the Robeson upper bound limit. The success of this blending technique has been confirmed by many researchers, and impressive results have been found for different polymer pairs.^{11–18} An improvement in the

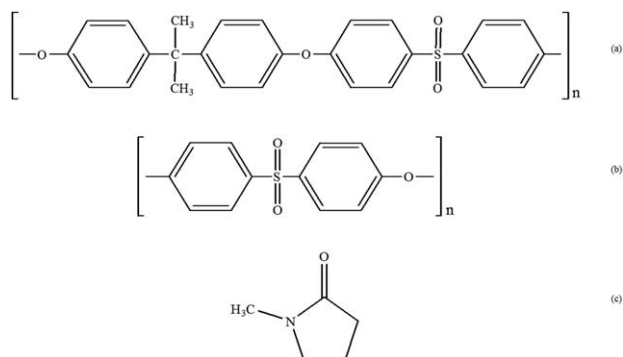


Figure 1. Chemical structures of (a) PSF, (b) PES, and (c) NMP.

permeability of O_2/N_2 gases was documented by Han *et al.*¹⁹ through the blending of poly(ether sulfone) (PES) and polyimide (PI) polymers. The polysulfone (PSF)/PI blend membranes reported by Basu *et al.*²⁰ showed improved separation performance of CO_2/CH_4 gas. The membranes were thermally stable and able to withstand harsh operating conditions of temperature and pressure. The PSF/PI blend membranes were also investigated by Rafiq *et al.*,²¹ and it was deduced that the PSF/PI blend presented superior thermal stability and separation performance in terms of CO_2 permeability and CO_2/CH_4 selectivity. These aforementioned studies demonstrated the blending of PSF and PES with PIs. However, interestingly, PSF/PES polymer blend membranes have not been reported in the literature for gas-separation applications to the best of our knowledge. PSF is a glassy polymer having a high plasticization resistance up to more than 50 bar with moderate separation performance and good thermal, chemical, and mechanical stabilities.²² PES is a high-performance glassy polymer with superior thermal, chemical, and mechanical properties.^{22,23} However, the plasticization pressure of PES is very low as compared to that of PSF.⁵ Moreover, it is a low-cost product compared to PSF. Thus, it seems very attractive to blend PSF and PES to compensate for these performance, plasticization, price, and stability limitations.

Therefore, in this study, we focused on the development of dense flat-sheet membranes consisting of PSF/PES blend. The effects of the polymer blend ratio on the morphology, thermal stability, polymer/polymer interaction, miscibility, and gas-transport properties of the synthesized membranes were studied. The synthesized PSF/PES blend membranes were characterized, and their physicochemical and gas-permeation properties were compared with those of individual polymers.

EXPERIMENTAL

Chemicals

PSF (Udel P-1800) in powdered form was supplied by Solvay Advanced Polymers, L.L.C. It had a glass-transition temperature (T_g) of 185°C . PES (ULTRASON E-6020P) in the form of flakes was purchased from BASF Germany. Its reported T_g was 225°C . The solvent *N*-methyl-2-pyrrolidone (NMP) used for this study was acquired from Merck with a reported purity of 99.99%. Figure 1 shows the chemical structures of the polymers and solvent used in this study.

Membrane Synthesis

The PSF and PES polymers were dried for 24 h at 90°C before use. Duran laboratory bottles were used to prepare the casting solution by the addition of 20% (w/w on the basis of the solvent) polymers in the NMP solvent. The mixture was gently stirred by a magnetic stirrer in a closed container for 24 h at room temperature until a thoroughly mixed, clear, viscous solution was obtained; this solution was allowed to stand for another 2 h to remove the air bubbles formed during the mixing process. To remove the entrapped air bubbles, the mixture was placed for 30 min in a sonication bath (Transsonic Digital S, Elma). The membranes were cast on a flat, smooth, dry, dust-free glass plate. The glass plate was washed with water and acetone to remove contaminants. Compressed air was applied to remove dust particles from the glass plate. The opening of the casting knife was adjusted to $200\ \mu\text{m}$ for membrane casting. The dope solution was poured onto the edge of the glass plate, and the casting knife was passed over the solution to form a uniform membrane layer. The prepared film was left to dry for 2–4 h before it was dried in the oven. The cast films were placed for 24 h at 90°C in a vacuum oven to evaporate the moisture and solvent. The synthesized membrane samples were secured for further characterization. Table I shows the description of the blend membranes along with the composition of the dope solution.

Membrane Characterization

Differential Scanning Calorimetry (DSC) Analysis. The T_g values of the pure and polymer blend membrane samples were examined by a Mettler-Toledo model DSC-1 instrument to evaluate the rigidity of the polymer chains and the miscibility of the blends. Samples were cut into small pieces with an average weight of 5–10 mg. The thermal scans were performed from 0 to 250°C under nitrogen flow with a heating rate of $10^\circ\text{C}/\text{min}$.

Field Emission Scanning Electron Microscopy (FESEM).

FESEM was used to examine the membrane morphology. For surface imaging, random specimens were taken from the membranes and observed through FESEM (Zeiss SUPRATM 55VP). For the cross-sectional images, membrane samples were dipped in liquid nitrogen for at least 30 s and fractured. Finally, the samples were mounted on a circular stainless steel sample holder for analysis.

Fourier Transform Infrared (FTIR).

In this study, the interaction between two polymers was analyzed by FTIR spectroscopy. A PerkinElmer Spectrum One FTIR spectrometer equipped with Spectra One software for analysis was used to observe the FTIR spectra in the wavelength range $400\text{--}4000\ \text{cm}^{-1}$. Membrane

Table I. Description of the Synthesized Membranes

Sample	PSF (wt %)	PES (wt %)	Name
1	100	0	PSF
2	80	20	PSF/PES (80–20)
3	50	50	PSF/PES (50–50)
4	20	80	PSF/PES (20–80)
5	0	100	PES

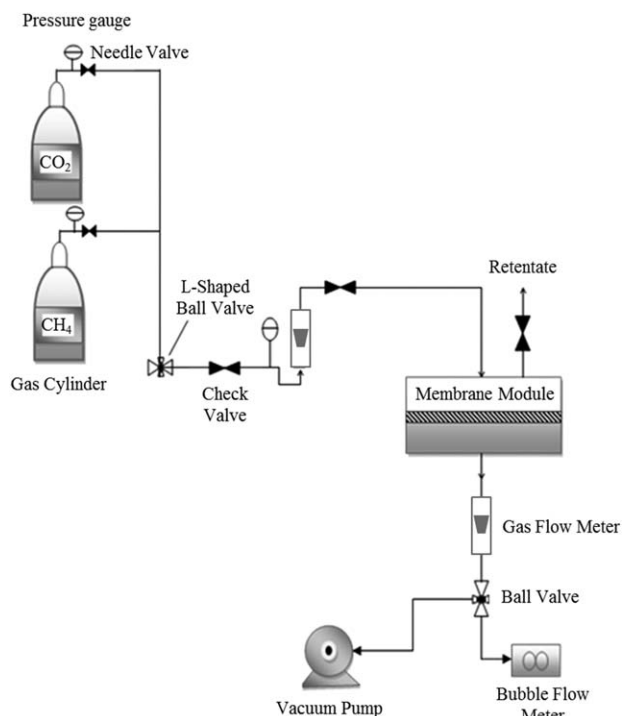


Figure 2. Schematic diagram of the membrane gas permeation unit.

samples were placed in a sample cell, and the spectrum was acquired by the coaddition of 20 scans at a resolution of 4 cm^{-1} under transmittance mode.

Thermogravimetric Analysis (TGA). The thermal stability and volatiles (moisture and solvents) were analyzed by a PerkinElmer TGA-1 instrument. We prepared the membrane samples by cutting small pieces and weighing 5–10 mg in a pan. TGA runs were performed from 30 to 800°C at a constant heating rate of $10^\circ\text{C}/\text{min}$ under a nitrogen atmosphere.

Gas Permeation

The separation performance of flat-sheet membranes was evaluated with a membrane gas-permeation unit, as shown in Figure 2. The unit consisted of pure gas feed tanks for CO_2 and CH_4 gases purchased from MOX-Linde Gases Sdn, pressure gauges for regulating the required pressure, gas flow meters for the required flow rate, a bubble flow meter for the permeate flow rate, a vacuum pump, and a dead-end membrane test module with an effective area of 14.54 cm^2 for membrane

permeation. The membrane test cell consisted of stainless steel paired disks, between which a membrane could be placed. Two O-ring seals were applied to prevent the leakage of gases from the membrane module. The entry of the gas was perpendicular to the membrane surface. A perforated polypropylene sheet and mesh were placed under the membrane to serve as a support. The top and bottom half of the cells were joined together by eight bolts and nuts, and the retentate valve was closed throughout the experiment. The schematic diagram of the membrane module is given in Figure 2. Before we started the experiments, the unit was vacuumed for 10 min to evacuate the residual gases. Feed gases with different feed pressures, that is, 2, 4, 6, 8, and 10 bar, were allowed to pass through the membrane. The permeate flow rate was recorded by a bubble flow meter because it provided a more accurate measurement of low flow rate ($<100\text{ mL}/\text{min}$) than a digital flow meter.²⁴ Because the weight of the bubble was negligible, the velocity of the bubble would have been equal to the velocity of the gas permeating through the membrane. The time required by the gas bubble to pass through a specific volume (2 mL) was recorded by a stopwatch to determine the volumetric flow rate. The permeance of species i (P_i) was calculated by the following equation²⁴:

$$\frac{P_i}{l} = \frac{Q_i \cdot 273}{T_i \cdot A \cdot \Delta p_i} \quad (1)$$

where Q_i is the volumetric flow rate of the permeate gas (cm^3/s), T_i is the absolute temperature (K), A is the effective area of the membrane (cm^2), Δp_i is the differential partial pressure across the membrane (cmHg), and l is the thickness of the membrane (cm). The permeance was reported in gas-permeation units (GPU).

We calculated the ideal selectivity of the membrane (α) with the ratio of the permeance values of CO_2 and CH_4 (P_{CO_2} and P_{CH_4} , respectively) as follows:

$$\alpha = \frac{P_{\text{CO}_2}}{l} / \frac{P_{\text{CH}_4}}{l} \quad (2)$$

RESULTS AND DISCUSSION

DSC Analysis of the Polymer Blends

The criteria of polymer miscibility includes obtaining a single T_g in a polymer solution; this indicates the miscibility at a molecular level.²⁵ Moreover, a single T_g confirms the homogeneous distribution of polymer chains in polymer films. In a phase-separated blend, two or more T_g values are observed, and usually, a compatibility agent is needed to form a compatible dope solution. The T_g values of the PSF/PES blend membranes

Table II. Summary of the TGA and DSC Analyses of the PSF/PES Blend Membranes

PSF (wt %)	PES weight (wt %)	Degradation onset temperature ($^\circ\text{C}$)	T_d ($^\circ\text{C}$)	T_g ($^\circ\text{C}$)
100	0	495.88	550.09	178.55
80	20	513.44	551.37	188.71
50	50	515.16	557.08	198.21
20	80	511.07	549.42	209.46
0	100	522.70	579.15	220.41

T_d , maximum degradation temperature.

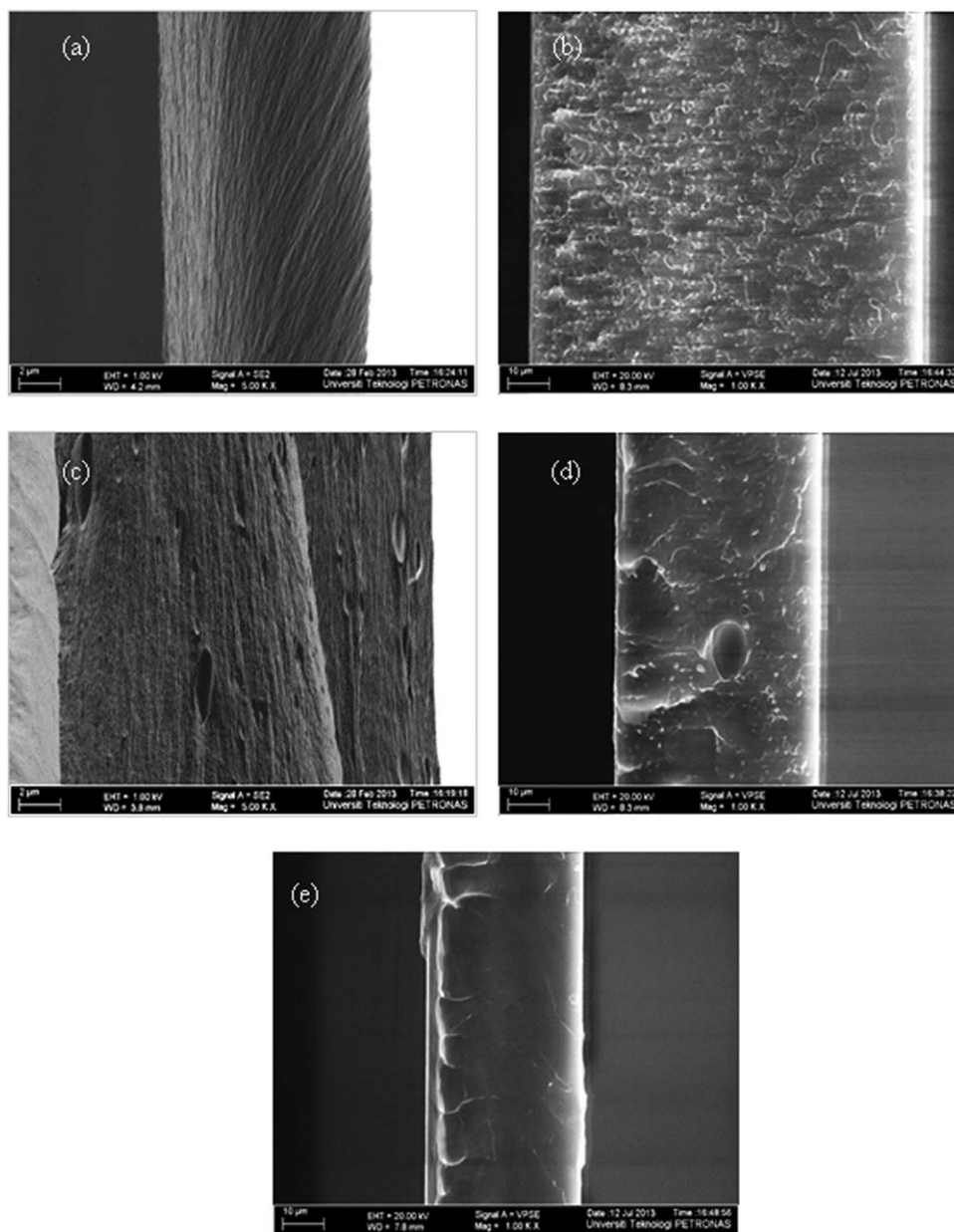


Figure 3. Cross-sectional images of the PSF/PES blend membranes: (a) PSF, (b) PSF/PES (80-20), (c) PSF/PES (50-50), (d) PSF/PES (20-80), and (e) PES.

is shown in Table II. For all of the membranes, a distinct T_g was observed; this was an indication of good interactions between the polymers. The T_g of the blend fell between those of the individual polymers. With an increase in the PES fraction in polymer matrix, the T_g of the blend increased uniformly, as shown in Table II, because of the higher T_g of PES. This indicated the improved stability of the blend. The miscibility of the PSF/PES blend in the DCM solvent over the entire composition range was reported by Linares and Acosta.²⁶ PSF/PI and PES/PI miscible blend membranes were also prepared by Rafiq *et al.*²¹ and Kapantaidakis *et al.*,²⁷ respectively.

Morphology of the Blend Membranes

Figure 3 shows cross-sectional images of the PSF/PES blend membranes. The morphologies of the blend membranes were

also compared with those of the parent polymers. All of the membranes had regularly packed, dense, rigid structures in the cross section with no pore formation. The cross-sectional images indicated that the PSF/PES blend was miscible and miscibility was achieved at a microscopic level. There was no phase separation in the surface and cross sections of the blend membranes. It is important to mention the concept of polymer miscibility in the polymer blends. The morphology of the polymer blends was affected by the intermolecular forces of the polymers. Generally, polymer blends are categorized as miscible blends and immiscible blends.²⁸ Miscible blends show a homogeneous morphology, whereas phase-separated blends are heterogeneous in nature. The morphologies of the PSF/PES and PES/PSF blend membrane presented the miscibility of this polymer pair. The surface morphology provided an indication of the

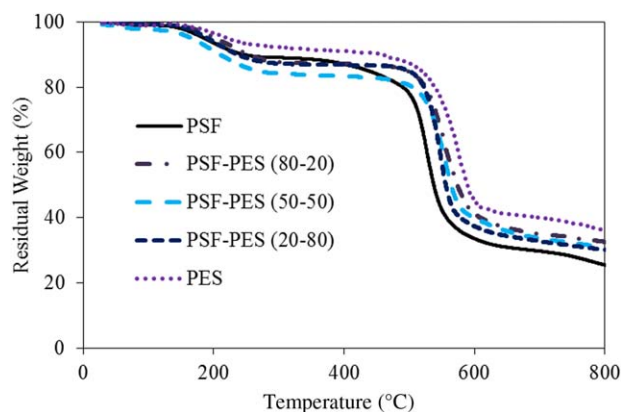


Figure 4. TGA of the PSF/PES blend membranes. [Color figure can be viewed in the online issue, which is available at wileyonlinelibrary.com.]

homogeneity of the PSF/PES blend. Homogeneous miscible blends, such as PSF/PI blend membranes, were also reported by Dorosti *et al.*²⁹

TGA

Figure 4 shows the TGA results of the PSF/PES blend membranes. The pure PSF and PES membranes are also shown for the comparative analysis. The initial weight loss below 200°C corresponded to the removal of moisture and solvent; this was less than 4–6%. For the pure PSF membrane, the degradation onset temperature was 495.88°C, and thermal degradation continued to a temperature of 550.09°C. Conversely, the initial degradation temperature of the pure PES membrane was noted to be 522.70°C, and the final degradation temperature was found to be 579.15°C. The degradation behavior of the blend membranes was between that of the pure polymers, and the blending of PES in the PSF matrix improved the thermal stability of the blend membranes. The stability of the PSF/PES (80–20) blend membrane improved from 495.88 to 513.44°C with the addition of 20% PES, whereas an addition of 50% PES enhanced the thermal degradation onset temperature to 515.16°C, and the degradation end temperature was observed to increase to 557.08°C.

The TGA curve of PSF/PES (20–80) with a high PES concentration deviated slightly from the expected behavior, and the degradation onset temperature fell to 511.07°C. This might have been due to interaction between the two polymers. The TGA results show a good agreement with previously reported studies.^{30,31} All of the blend membranes showed a single degradation peak in the TGA graph; this showed the miscibility of the PSF/PES blend in the whole compositional range. Dorosti *et al.*²⁹ studied PSF/PI over the entire compositional range and found a miscible blend. The blend membranes showed a uniform behavior in weight loss, and the stability of the blend membranes was between those of the pure polymers. Table II shows the TGA summary of the blend membranes.

FTIR Analysis of the Blend Membranes

The surface chemistry of the blend membranes was analyzed by FTIR spectroscopy. Figure 5 shows the FTIR spectra of the PSF/PES blend membranes. The spectral behavior of the blend membranes showed a few shifts; for example, in the PSF/PES

(80–20) blend membrane, benzene ring stretching was noticed at 1479.82–1599.30 cm^{-1} . The shift from 1590 to 1599 cm^{-1} was quite significant and broad. Moreover, the shift in the C–SO₂–C band from 1258.72 to 1275.84 cm^{-1} was also noticeable. These shifts might have been due to hydrogen bonding between the two polymers.³¹ In all of the membranes, the C–H stretching peak of benzene appeared in the range 3093–3095 cm^{-1} . In all of the blend membranes, the appearance of a distinct and broad peak in the range 3448–3460 cm^{-1} might have been due to hydrogen bonding; this indicated that the PSF/PES blend was a miscible and compatible blend.

The FTIR analysis of the synthesized membranes proved the existence of physical interaction between the blend polymers. There were no signs of intermediate formation, crosslinking, or chemical interaction between the polymers during the blending process.

Gas-Permeation Studies

The permeation of the CO₂ and CH₄ gases through the PSF/PES blend membranes was recorded at a pressure of 2–10 bar. Figures 6 and 7 show the CO₂ and CH₄ permeation behaviors, respectively, of the blend membranes, and their corresponding selectivity is shown in Figure 8. The performance of blend membranes was compared with the pure polymeric membranes with PSF as a base polymer. The PSF membrane had the highest value of CO₂ and CH₄ permeability and the lowest value of selectivity. PES membrane had the lowest value of CO₂ and CH₄ permeability and the highest value of selectivity. The blend membranes showed performances between these two parent polymers. Thus, the addition of PES to the PSF matrix caused a decrease in the permeability of the permeating gases, as expected. As the percentage of PES increased, the permeability of the blend membrane fell, and there was an almost 50% decrease in the permeability of CO₂ gas in the PSF/PES (20–80) membrane when compared to the pure PSF membrane at 10 bar. The feed pressure had a significant effect on the

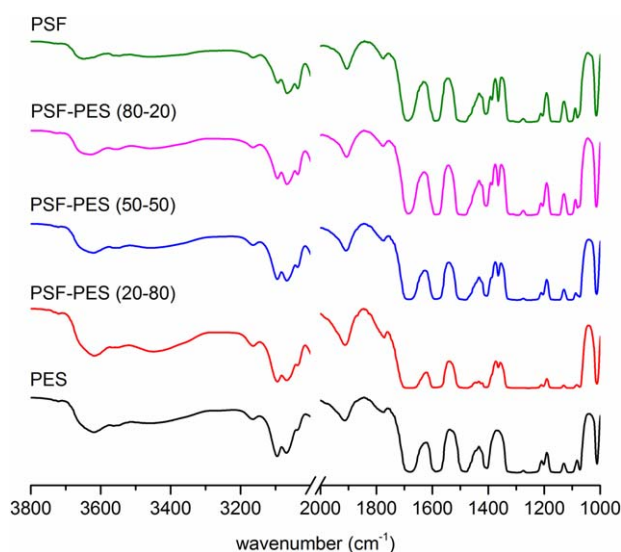


Figure 5. FTIR spectra of the PSF/PES blend membranes. [Color figure can be viewed in the online issue, which is available at wileyonlinelibrary.com.]

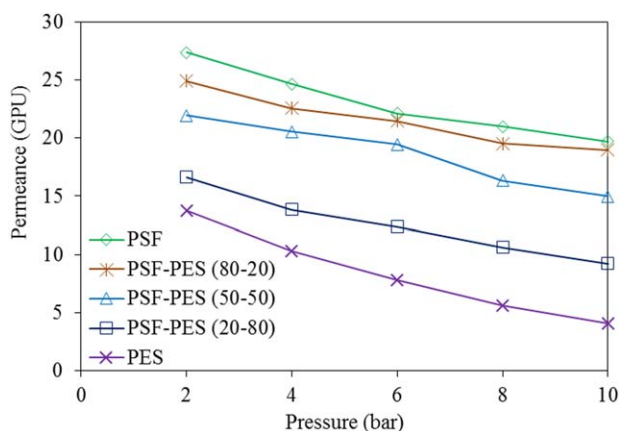


Figure 6. CO₂ permeability of the PSF/PES blend membranes. [Color figure can be viewed in the online issue, which is available at wileyonlinelibrary.com.]

permeability of the membranes. An increase in the pressure led to a gradual fall in the permeabilities of CO₂ and CH₄ because of the competitive adsorption of gas molecules. At low pressure, the permeability of all of the membranes was higher compared to the permeability at higher pressures. For example, the CO₂ permeability of the PSF membrane was 27.41 GPU at 2 bar and 19.71 GPU at 10 bar; this accounted for a 28% reduction in the permeability. In the blend membranes, the PSF/PES (20-80) membrane underwent a maximum reduction of 70% in CO₂ permeability from 13.76 GPU at 2 bar to 4.03 GPU at 10 bar. In glassy polymers, gas transport by a diffusion mechanism is dominant because they are rigid and hard in structure. A high energy is needed to make a diffusion jump. In all of the membranes, the permeability of CO₂ was higher than that of CH₄. The relative sizes of CO₂ and CH₄ favored a high permeation of CO₂. The kinetic diameter of CO₂ (3.3 Å) was smaller than that of CH₄ (3.8 Å); this may have also led to a greater diffusivity compared to that of CH₄ gas. These observations identified characteristics of glassy polymers, and their blend also represented the same behavior.²² Similar findings were also reported by other researchers.^{14,20–22,29}

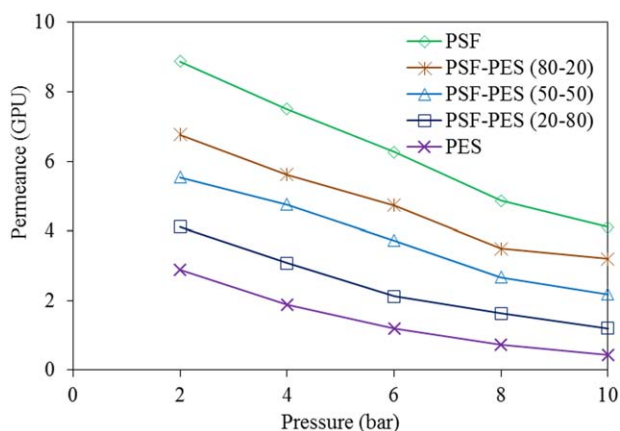


Figure 7. CH₄ permeability of the PSF/PES blend membranes. [Color figure can be viewed in the online issue, which is available at wileyonlinelibrary.com.]

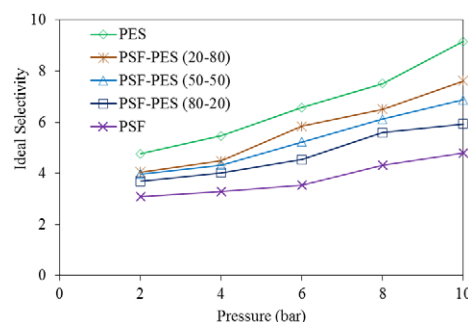


Figure 8. Ideal selectivity of the PSF/PES blend membranes. [Color figure can be viewed in the online issue, which is available at wileyonlinelibrary.com.]

Similarly, the selectivity of the PSF/PES blend membranes is portrayed in Figure 8. The selectivity of the blend membranes showed an increasing trend with respect to pressure. The highest selectivity was obtained in the pure PES membrane, and the lowest was obtained in the pure PSF membrane. The internal structure of the membranes was responsible for such behavior, that is, the rigidity of PES and the relative softness of the PSF membranes, as discussed in the Membrane Characterization section. The separation performance of the blend membranes was between those of the parent polymers. The high concentration of PES favored the separation of CO₂/CH₄, and an improved ideal selectivity was observed. The highest influence was seen in the PSF/PES (20-80) membrane, where the ideal selectivity improved from 3.54 for pure PSF to 5.84 for PSF/PES (20:80) at 6 bar; this accounted for a 65% improvement in the ideal selectivity as compared to that of the base PSF membrane. The pressure had a positive effect on the improvement of ideal selectivity, and the trend grew regularly with increasing pressure. The pure PES membrane showed an enhancement of 92.44% in ideal selectivity from 4.76 at 2 bar to 9.16 at 10 bar; this was a result of the reduced permeability, as discussed earlier in this section. In the blend membranes, the PSF/PES (20-80) membrane underwent a maximum enhancement of 88.36% in ideal selectivity from 4.04 at 2 bar to 7.61 at 10 bar.

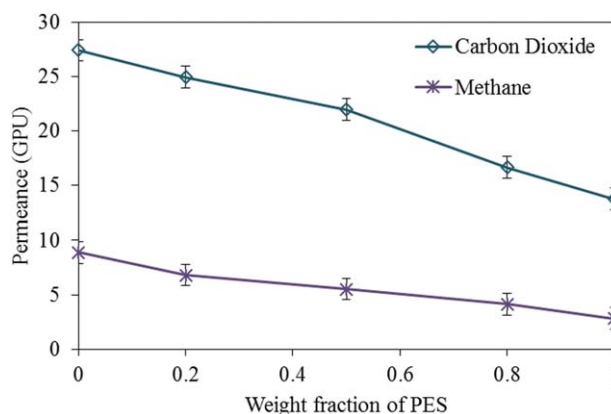


Figure 9. Effect of the PES weight fraction on the permeability of the CO₂ and CH₄ gases at 2 bar and 25°C. [Color figure can be viewed in the online issue, which is available at wileyonlinelibrary.com.]

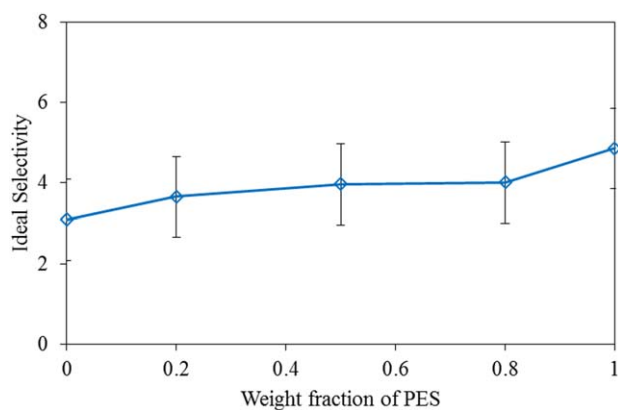


Figure 10. Effect of the PES weight fraction on the selectivity of the PSF/PES membranes at 2 bar and 25°C. [Color figure can be viewed in the online issue, which is available at wileyonlinelibrary.com.]

Effect of the PES Fraction on the Transport Properties of the PSF/PES Blend Membranes

The blend ratio of the synthesized membranes had a significant effect on the gas-permeation behavior of the membranes. It is worth mentioning that the performance of the PSF membrane improved with increasing concentration of PES in the PSF matrix. The internal structure of PES was more tightly packed [Figure 3(e)] as compared to that of the PSF membrane [Figure

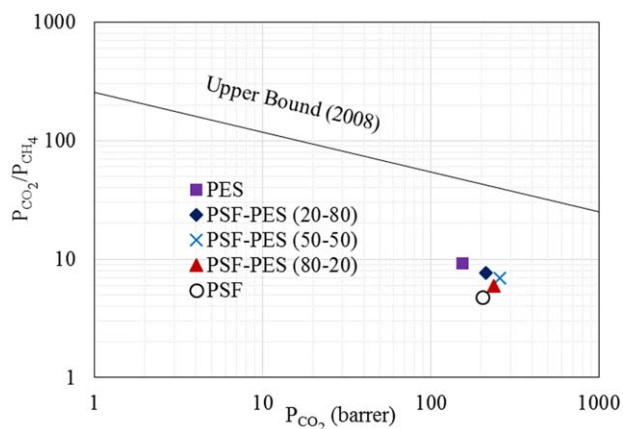


Figure 11. Performance of the PSF/PES blend membranes on the Robeson upper bound line. [Color figure can be viewed in the online issue, which is available at wileyonlinelibrary.com.]

3(a)], and it had a superior gas-separation performance. Thus, the passage of gas molecules was hindered because of the internal structure of PES; this resulted in a decreased permeability and increased selectivity.³¹ The PSF membrane was relatively soft compared to PES, and the diffusion of gas molecules was easier. Figure 9 shows the permeability of CO₂ and CH₄ against different concentrations of PES at 2 bar and 25°C. With

Table III. Comparison of This Study with the Literature for CO₂/CH₄ Separation

Polymer	Additive	Membrane type	Feed pressure (bar)	Ideal selectivity	Reference
PSF	—	Asymmetric	3	1.80	33
PSF	PVP (5 wt %)	Asymmetric	3	1.00	33
PES	—	Dense	10	1.61	34
PES	MEA	Dense	10	1.92	34
PVC	SBR	Dense	2	7.12	35
PVC	SBR	Dense MMM with 30% zeolite loading	2	0.58	35
PES	—	Dense	10	1.55	36
PES	IL	Dense	10	2.27	36
PBI	Matrimid	Hollow fiber	10	5.04	16
PES	—	Asymmetric	2	5.46	37
PES	CNT	Asymmetric MMM	2	4.97	37
PSF	PI	Dense	5	4.80	29
PSF	PI	Dense MMM with 20 wt % ZSM-5	5	2.90	29
PU	PVAc	Dense	10	8.81	11
PEBAX	PDMS/PESPEG	Dense	4	10.8	38
PES	DEA	Dense MMM with 10% CMS loading	10	20.21	39
PES	PVAc	Dense	10	1.40	40
PSF	—	Dense	10	4.80	This study
PES	—	Dense	10	9.13	This study
PSF	PES	Dense	10	7.60	This study

PVP = polyvinylpyrrolidone; PVC = polyvinyl chloride; PBI = polybenzimidazole; PU = polyurethane; PEBAX, polyether-block-amide; PVAc = polyvinyl acetate; DEA = diethanolamine; PDMS = poly(dimethyl siloxane); MEA = monoethanolamine; SBR = Styrene-Butadiene-Rubber; IL = ionic liquid; CNT = Carbon nanotube; CMS = carbon molecular sieve; ZSM-5 = Zeolite Socony Mobil-5.

increasing PES concentration, the permeability decreased and the selectivity increased because of the inherently low permeability and high selectivity of the PES polymer. The CO₂ permeability of the blend membranes was reduced by 9, 19.85, 39.26, and 50% as the concentration of PES in the PSF matrix was increased to 20, 50, 80, and 100%, respectively. A similar pattern for CH₄ was also observed. The permeability in glassy polymers was related to the fractional free volume (FFV) of the polymers (the volume not occupied by the polymer); this, in turn, depended on the polymer density.³² PES was denser compared to PSF; thus, it provided a lower FFV than PSF. Therefore, a high PES concentration resulted in a decreased FFV, decreased permeability, and ultimately increased selectivity. Moreover, the permeability of CO₂ was affected more than that of CH₄ because of the decreased FFV. The selectivity of the blend membranes against different concentrations of PES at 2 bar and 25°C is shown in Figure 10. As the fraction of PES increased, a better selectivity was achieved. At higher concentrations of PSF and PES in blend, their respective individual behaviors were dominant. In the middle range of the blend, the selectivity was lower than accounted for by the simple additive rule because of the increased interaction between the polymers. Similar effects of the permeability and selectivity of polymers of intrinsic microporosity (PIM-1)/Matrimid blend membranes were noticed by Yong *et al.*³²

The gas-permeation performance of the blend membranes justifies them to be considered as a new membrane material for the optimization of cost and separation performance. From PSF point of view, the addition of PES offered a remarkable improvement in the separation performance. Also, the high cost of PSF can be reduced through the blending of PES with the PSF matrix because if the same or superior performance can be obtained by the blending of a low cost material, the pure PSF membrane is overly expensive. From PES point of view, the blending of PSF provides a reasonable combination of permeability without a sacrifice of the selectivity. Although the investigation of the plasticization of these membranes was beyond the scope of this study, it is believed that the plasticization pressure of PSF/PES blend membranes would have been improved from 20–25 bar (PES) to 35–40 bar, which falls within the operating pressure range of industrial membrane processes. Thus, the plasticization problem of PES membranes can be circumvented by the addition of PSF. Therefore, we concluded that the PSF/PES (50:50) blend membrane provided an optimal combination of cost, permeability, selectivity, thermal and mechanical stability, and plasticization resistance.

Comparison of This Study with the Literature

Table III shows the comparison of this study with different types of membranes used for CO₂/CH₄ separation. This comparison includes mixed matrix membrane (MMM), ionic-liquid-supported polymeric membranes, polymer blend membranes, and asymmetric membranes prepared with different polymeric materials. In comparison to the literature values, the PSF/PES blend can be considered as a novel material for gas-separation membrane development with its improved permeability, selectivity, and thermal stability. Figure 11 shows the performance of the synthesized blend membranes on the Robeson upper bound line.⁴¹

CONCLUSIONS

In this article, we have summarized the investigation of PSF/PES blend membranes synthesized by solvent evaporation process. PSF and PES were chosen as blend components to compensate for the thermal, mechanical, and gas-separation properties of the individual polymers. The PSF/PES blend was found to be miscible in all of the compositions with probable hydrogen bonding, as indicated by the FESEM, DSC, FTIR spectroscopy, and TGA results. The morphology of the blend membranes was homogeneous with no pore formation. The thermal stability of the blend membranes fell between those of the individual polymers and was increased with increasing concentration of highly stable PES in the PSF matrix. We observed that the permeation of CO₂ and CH₄ gases followed the typical behavior of glassy polymers; that is, the permeability decreased and the selectivity increased with increasing pressure. The permeability and selectivity values of the polymer blend membranes were between those of the individual polymer membranes. The addition of PES in the PSF membranes enhanced the separation performance of the blend membranes and, consequently, a 65% increment in the selectivity was observed in the PSF/PES membranes. In general, these blend membranes could be considered as a potential development in optimizing the cost and performance of PSF/PES membranes.

ACKNOWLEDGMENTS

The authors gratefully acknowledge the Ministry of Education of Malaysia for providing funds (contract grant number FRGS-0153AB-I68) and the Universiti Teknologi Petronas for providing financial support and equipment facilities through the University Internal Research Fund (contract grant number URIF-0153AA-B21).

REFERENCES

1. Bernardo, P.; Clarizia, G. *Chem. Eng.* **2013**, *32*, 1999.
2. Chung, T. S.; Jiang, L. Y.; Li, Y.; Kulprathipanja, S. *Prog. Polym. Sci.* **2007**, *32*, 483.
3. Baker, R. W.; Low, B. T. *Macromolecules* **2014**, *47*, 6999.
4. Robeson, L. M. *J. Membr. Sci.* **1991**, *62*, 165.
5. Ismail, A. F.; Lorna, W. *Sep. Purif. Technol.* **2002**, *27*, 173.
6. Aroon, M.; Ismail, A.; Matsuura, T.; Montazer-Rahmati, M. *Sep. Purif. Technol.* **2010**, *75*, 229.
7. Sanders, D. F.; Smith, Z. P.; Guo, R.; Robeson, L. M.; McGrath, J. E.; Paul, D. R.; Freeman, B. D. *Polymer* **2013**, *54*, 4729.
8. Mannan, H. A.; Mukhtar, H.; Murugesan, T.; Nasir, R.; Mohshim, D. F.; Mushtaq, A. *Chem. Eng. Technol.* **2013**, *36*, 1838.
9. Nasir, R.; Mukhtar, H.; Man, Z.; Mohshim, D. F. *Chem. Eng. Technol.* **2013**, *36*, 717.
10. Mohshim, D. F.; Mukhtar, H.; Man, Z.; Nasir, R. *J. Eng.* **2013**, *2013*, 7.
11. Semsarzadeh, M. A.; Ghalei, B. *J. Membr. Sci.* **2012**, *401*, 97.

12. Patrício, P. S. O.; de Sales, J. A.; Silva, G. G.; Windmüller, D.; Machado, J. C. *J. Membr. Sci.* **2006**, *271*, 177.
13. de Sales, J. A.; Patrício, P. S. O.; Machado, J. C.; Silva, G. G.; Windmüller, D. *J. Membr. Sci.* **2008**, *310*, 129.
14. Khan, A. L.; Li, X.; Vankelecom, I. F. J. *J. Membr. Sci.* **2011**, *380*, 55.
15. Hosseini, S. S.; Teoh, M. M.; Chung, T. S. *Polymer* **2008**, *49*, 1594.
16. Hosseini, S. S.; Peng, N.; Chung, T. S. *J. Membr. Sci.* **2010**, *349*, 156.
17. Rafiq, S.; Man, Z.; Maulud, A.; Muhammad, N.; Maitra, S. *Sep. Purif. Technol.* **2012**, *90*, 162.
18. Car, A.; Stropnik, C.; Yave, W.; Peinemann, K. V. *J. Membr. Sci.* **2008**, *307*, 88.
19. Han, J.; Lee, W.; Choi, J. M.; Patel, R.; Min, B. R. *J. Membr. Sci.* **2010**, *351*, 141.
20. Basu, S.; Cano-Odenaa, A.; Vankelecom, I. F. J. *Sep. Purif. Technol.* **2010**, *75*, 15.
21. Rafiq, S.; Man, Z.; Maitra, S.; Maulud, A.; Ahmad, F.; Muhammad, N. *Korean J. Chem. Eng.* **2011**, *28*, 2050.
22. Kapantaidakis, G.; Kaldis, S.; Dabou, X.; Sakellaropoulos, G. *J. Membr. Sci.* **1996**, *110*, 239.
23. Sridhar, S.; Smitha, B.; Aminabhavi, T. M. *Sep. Purif. Rev.* **2007**, *36*, 113.
24. Rafiq, S. Ph.D. Thesis, Universiti Teknologi Petronas, Tronoh, **2013**.
25. Barlow, J. W.; Paul, D. R. *Polym. Eng. Sci.* **1981**, *21*, 985.
26. Linares, A.; Acosta, J. L. *J. Appl. Polym. Sci.* **2004**, *92*, 3030.
27. Kapantaidakis, G.; Koops, G.; Wessling, M. *Desalination* **2002**, *145*, 353.
28. Robeson, L. M. *Ind. Eng. Chem. Res.* **2010**, *49*, 11859.
29. Dorosti, F.; Omidkhah, M. R.; Pedram, M. Z.; Moghadam, F. *Chem. Eng. J.* **2011**, *171*, 1469.
30. Rafiq, S.; Man, Z.; Maitra, S.; Muhammad, N.; Ahmad, F. *J. Appl. Polym. Sci.* **2012**, *123*, 3755.
31. Mannan, H. A.; Mukhtar, H.; Murugesan, T. *Appl. Mech. Mater.* **2015**, *699*, 325.
32. Yong, W. F.; Li, F. Y.; Xiao, Y. C.; Li, P.; Pramoda, K. P.; Tong, Y. W.; Chung, T. S. *J. Membr. Sci.* **2012**, *407*, 47.
33. Moradihamedani, P.; Ibrahim, N. A.; Yunus, W. M. Z. W.; Yusof, N. A. *J. Appl. Polym. Sci.* **2013**, *130*, 1139.
34. Nasir, R.; Mukhtar, H.; Man, Z.; Mohshim, D. F. *Int. J. Chem. Mater. Sci. Eng.* **2013**, *7*, 38.
35. Moghadassi, A. R.; Rajabi, Z.; Hosseini, S. M.; Mohammadi, M. *Arab. J. Sci. Eng.* **2014**, *39*, 605.
36. Mohshim, D. F.; Mukhtar, H.; Man, Z. *Key Eng. Mater.* **2014**, *594*, 18.
37. Sudharto, J. P. *World Appl. Sci. J.* **2014**, *31*, 1512.
38. Reijerkerk, S. R.; Knoef, M. H.; Nijmeijer, K.; Wessling, M. *J. Membr. Sci.* **2010**, *352*, 126.
39. Nasir, R.; Mukhtar, H.; Man, Z.; Dutta, B. K.; Shaharun, M. S.; Abu Bakar, M. Z. *J. Membr. Sci.* **2015**, *483*, 84.
40. Hadi, S. H. A. A.; Mukhtar, H.; Mannan, H. A.; Murugesan, T. *Appl. Mech. Mater.* **2015**, *754*, 44.
41. Robeson, L. M. *J. Membr. Sci.* **2008**, *320*, 390.